Accepted Manuscript

Photophysical properties and photocytotoxicity of free and liposome-entrapped diazepinoporphyrazines on LNCaP cells under normoxic and hypoxic conditions

Ewelina Wieczorek, Dariusz T. Mlynarczyk, Malgorzata Kucinska, Jolanta Dlugaszewska, Jaroslaw Piskorz, Lukasz Popenda, Wojciech Szczolko, Stefan Jurga, Marek Murias, Jadwiga Mielcarek, Tomasz Goslinski

PII: S0223-5234(18)30201-0

DOI: 10.1016/j.ejmech.2018.02.064

Reference: EJMECH 10241

To appear in: *European Journal of Medicinal Chemistry*

Received Date: 19 December 2017

Revised Date: 5 February 2018

Accepted Date: 20 February 2018

Please cite this article as: E. Wieczorek, D.T. Mlynarczyk, M. Kucinska, J. Dlugaszewska, J. Piskorz, L. Popenda, W. Szczolko, S. Jurga, M. Murias, J. Mielcarek, T. Goslinski, Photophysical properties and photocytotoxicity of free and liposome-entrapped diazepinoporphyrazines on LNCaP cells under normoxic and hypoxic conditions, *European Journal of Medicinal Chemistry* (2018), doi: 10.1016/j.ejmech.2018.02.064.

Graphical Abstract

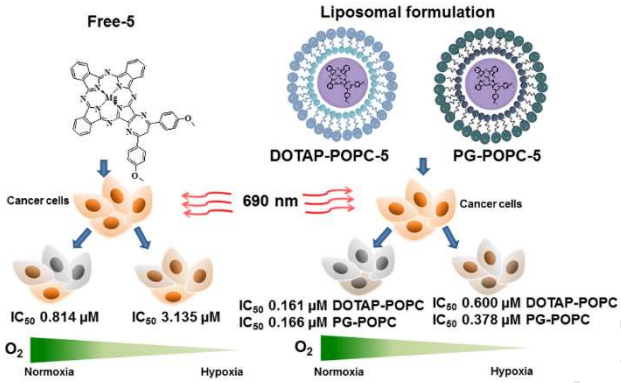

Photophysical properties and photocytotoxicity of free and liposome-entrapped diazepinoporphyrazines on LNCaP cells under normoxic and hypoxic conditions

Ewelina Wieczorek[a], Dariusz T. Mlynarczyk[a], Malgorzata Kucinska[b], Jolanta Dlugaszewska[c], Jaroslaw Piskorz[d], Lukasz Popenda[e], Wojciech Szczolko[a], Stefan Jurga[e,f], Marek Murias[b], Jadwiga Mielcarek[d], Tomasz Goslinski[a,*]

[a] *Department of Chemical Technology of Drugs, Poznan University of Medical Sciences, Grunwaldzka 6, 60-780 Poznan, Poland*

[b] *Department of Toxicology, Poznan University of Medical Sciences, Dojazd 30, 60-631 Poznan, Poland*

[c] *Department of Genetics and Pharmaceutical Microbiology, Poznan University of Medical Sciences, Swiecickiego 4, 60-780 Poznan, Poland*

[d] *Department of Inorganic and Analytical Chemistry, Poznan University of Medical Sciences, Grunwaldzka 6, 60-780 Poznan, Poland*

[e] *NanoBioMedical Centre, Adam Mickiewicz University, Umultowska 85, 61-614 Poznan, Poland*

[f] *Department of Macromolecular Physics, Adam Mickiewicz University, Umultowska 85, 61-614 Poznan, Poland*

Abstract

5,7-Diaryl-substituted symmetrical diazepinoporphyrazine and tribenzodiazepinoporphyrazine were synthesized and characterized using UV–Vis, MS MALDI, and various NMR techniques. The expected photosensitizing potentials of these porphyrazines were evaluated by measuring their abilities to generate singlet oxygen in organic solvents and by comparing them with that of the recently obtained dendrimeric G1-type diazepinoporhyrazine. Absorbance and fluorescence measurements were performed to study the aggregation properties of the novel macrocycles. The photocytotoxicity of tribenzodiazepinoporphyrazine towards LNCaP cells in its free form and after its incorporation into liposomes was examined using MTT assay under normoxic and hypoxic conditions. It is interesting that all tested liposome formulations maintained their phototoxic activity in hypoxia. Also, tribenzodiazepinoporphyrazine incorporated into liposomes revealed better photocytotoxic effect (IC_{50} values of 0.600 ± 0.357 μM and 0.378 ± 0.002 μM) than its free form (IC_{50} values

of 3.135 ± 0.156 μM). Following the *in vitro* experiments, the most promising liposomal formulation containing L-α-phosphatidyl-DL-glycerol for tribenzodiazepinoporphyrazine was found. Moreover, tribenzodiazepinoporphyrazine incorporated into liposomes containing 1,2-dioleoyl-3-trimethylammonium-propane (chloride salt) revealed moderate phototoxicity at 5×10^{-5} μM for antibacterial photodynamic therapy. It was established that an irradiation of planktonic bacterial strains significantly reduced CFUs of *Staphylococcus aureus* ATCC 25923 in comparison to tribenzodiazepinoporphyrazine containing L-α-phosphatidyl-DL-glycerol liposomes.

Keywords

diaminomaleonitrile, photocytotoxicity, porphyrazine, singlet oxygen, photodynamic activity

*Correspondence to: T. Goslinski, Department of Chemical Technology of Drugs, University of Medical Sciences, Grunwaldzka 6, 60-780, Poznan, Poland. Tel.: +48 61 854 66 31, fax: +48 61 854 66 39. E-mail: tomasz.goslinski@ump.edu.pl

1. Introduction

For the last 20 years, macrocyclization reactions of 1,4-diazepine-2,3-dicarbonitrile derivatives have led to a plethora of various porphyrazines with annulated rings of diazepine,[1-3] tetrahydrodiazepine,[4,5] and styryldiazepine[5-8]. Styryl-substituted diazepinoporphyrazines have been evaluated for their electronic properties, for the tendency for aggregation and photodegradation, singlet oxygen generation efficiency, and *in vitro* photodynamic activity at a nanomolar level against two oral squamous cell carcinoma cell lines.[5,7,8] 5,7-Diphenyl- and 5,7-di(4-*tert*-butylphenyl)-substituted diazepinoporphyrazines and tribenzodiazepinoporphyrazines have also been studied towards electronic[1-3,9,10] and electrochemical properties.[11,12]

Porphyrazine macrocycles seem to be suitable candidates for photodynamic therapy (PDT) for many reasons. They exhibit high generation quantum yields of singlet oxygen and have adequate light absorption spectra. Moreover, porphyrazines absorb light in the so-called therapeutic window in range 600-800 nm, where the tissues are the most permeable to such wavelengths. On the one hand, porphyrinoid photosensitizers are lipophilic and reveal high affinity to lipids, which seems beneficial, as cancer cells are often overexpressing LDL-receptors.[13] On the other hand, the high lipophilicity of porphyrinoids hampers their solubility in water and increases their tendency to form aggregates in polar solvents. This issue can be overcome by incorporation of photosensitizers into various pharmaceutical formulations, including liposomes proven as useful carriers.[14] Liposomes offer a huge advantage in lipophilic photosensitizer delivery, not only by enabling water-insoluble compound delivery but also in functionalization of the liposome membrane. The tunable charge of the carrier can also have a great effect on the effectiveness of the therapy. Photosensitizers like hydrophobic porphyrazines accumulate in liposomal membranes. In this regard, smaller porphyrazine macrocycles are preferred, as the thickness of membranes is limited thus making it impossible to incorporate bulky porphyrinoid structures.

To further address the issue of anticancer therapies, one of the characteristics of the cancer tissues such as hypoxia, must be taken into account. For many years until now, it is well known that tumor hypoxia has been a significant limitation of anticancer therapies, which depend on oxygen-mediated mechanisms such as radiation, photodynamic therapy as well as chemotherapy.[15] Although PDT has been found to be effective against the superficial tumor, the photodynamic efficacy for solid tumors, which are characterized by the hypoxic environment, is still challenging.[16] The rapid growth of the neoplasm cells and their increased

metabolism are factors triggering hypoxia,[17] which is a major problem in case of photodynamic therapy, as molecular oxygen is one of the three factors determining a successful treatment. The singlet oxygen ($^1O_2$) generated in type II photoreaction is still considered as the primary cytotoxic agent for PDT. Therefore, the low oxygen concentration may decrease the efficacy of photodynamic treatment to cancer cells.[18,19] To date, several strategies were designed to overcome tumor hypoxia in the context of PDT such as modification of the tumor microenvironment to ensure tissue re-oxygenation, the increase of intracellular oxygen concentration as well as the development of the photosensitizer, which may induce cytotoxic effects in environments of low molecular oxygen via type I photosensitization.[15,16,20] Thus, it is essential to develop photosensitizers which may exert therapeutic effects under both normoxia and hypoxia.

Currently, screening of photosensitizers during photodynamic therapy is mainly focused on normoxic condition. However, it should be noted that the median oxygenation in untreated tumors varies between approximately 0.3% and 4.2% oxygen and most tumors demonstrate median oxygen levels below 2%.[21] This range in tumor oxygenation depends on several factors, and hypoxic microregions are heterogeneously distributed within the tumor mass.[22] It is worth noting that many prostate and pancreatic tumors are strongly hypoxic.[21] Moreover, the hypoxia in prostate cancer is also related to advanced tumor stage, aggressive disease as well as increased resistance to androgen deprivation and radio- and chemotherapy.[23] Recently, we have reported the synthesis of diazepinoporphyrazine with G1-dendrimeric substituents and discussed its photophysical properties as well as singlet oxygen generation efficiency.[12] Herein, as an enhancement of our studies, we report the synthesis, physicochemical characterization, including absorption and emission properties, tendency to aggregation of magnesium(II) diazepinoporphyrazine and tribenzodiazepinoporhyrazine substituted in their C5 and C7 positions with 4-methoxyphenyl groups. Moreover, the anticancer potential of new porphyrazines was assessed in liposomal formulations in both normoxia and hypoxia conditions against prostate adenocarcinoma cells.

2. Results and discussion

2.1. Synthesis and characterization

Novel magnesium diazepinoporphyrazine substituted at C5 and C7 positions with 4-methoxyphenyl groups (**4**) was synthesized in two steps (Scheme 1). Firstly, the condensation reaction of diaminomaleonitrile (**1**) and 1,3-bis(4-methoxyphenyl)-1,3-propanedione (**2**) was

performed following the literature procedure,[9] and led to the novel 5,7-disubstituted-1,4-diazepine-2,3-dicarbonitrile (**3**). Subsequent macrocyclization reaction of **3** using magnesium *n*-butanolate in *n*-butanol according to the Linstead macrocyclization conditions[24] enabled the obtaining of symmetrical diazepinoporphyrazine **4** with 10% yield.[12] Tribenzodiazepinoporphyrazine (**5**) was synthesized following a similar procedure but with the addition of an excessive amount of 1,2-dicyanobenzene (ten-fold mol/mol excess to **3**). After extensive chromatography, macrocycle **5** was isolated in 3.5% yield.

To unambiguously identify the isolated macrocyclic products, NMR experiments were carried out. The ^{1}H NMR spectrum of **4** revealed two doublets at 8.56 ppm and 6.89 ppm assigned to 32 protons of phenyl rings, two broad doublets (^{2}J ~ 13 Hz) observed at 6.86 ppm and 6.07 ppm from C6-CH_2 eight geminal protons, and one singlet at 3.80 ppm resulting from all methoxy groups, 24 protons. It is worth mentioning that the presence of two doublets from C6-CH_2 geminal protons indicates that all diazepine rings of **4** are in the 6*H* tautomeric form.[1]

Similarly, for **5**, two doublets corresponding to the aromatic protons of 4-methoxy substituents were detected at 8.55 ppm and 7.21 ppm in the ^{1}H NMR spectrum. Only one singlet in the spectrum at 3.94 ppm was assigned to methoxy group protons. A very weak and broad signal corresponding to diazepine ring protons was observed at 4.59 ppm. Four signals at 9.46, 9.38, 8.27, 8.24 ppm were assigned to protons at annulated benzene rings. The assignments of ^{1}H resonances were confirmed by ^{1}H-^{1}H COSY, ^{1}H-^{13}C HMBC, and ^{1}H-^{13}C HSQC experiments (see Supporting Information).

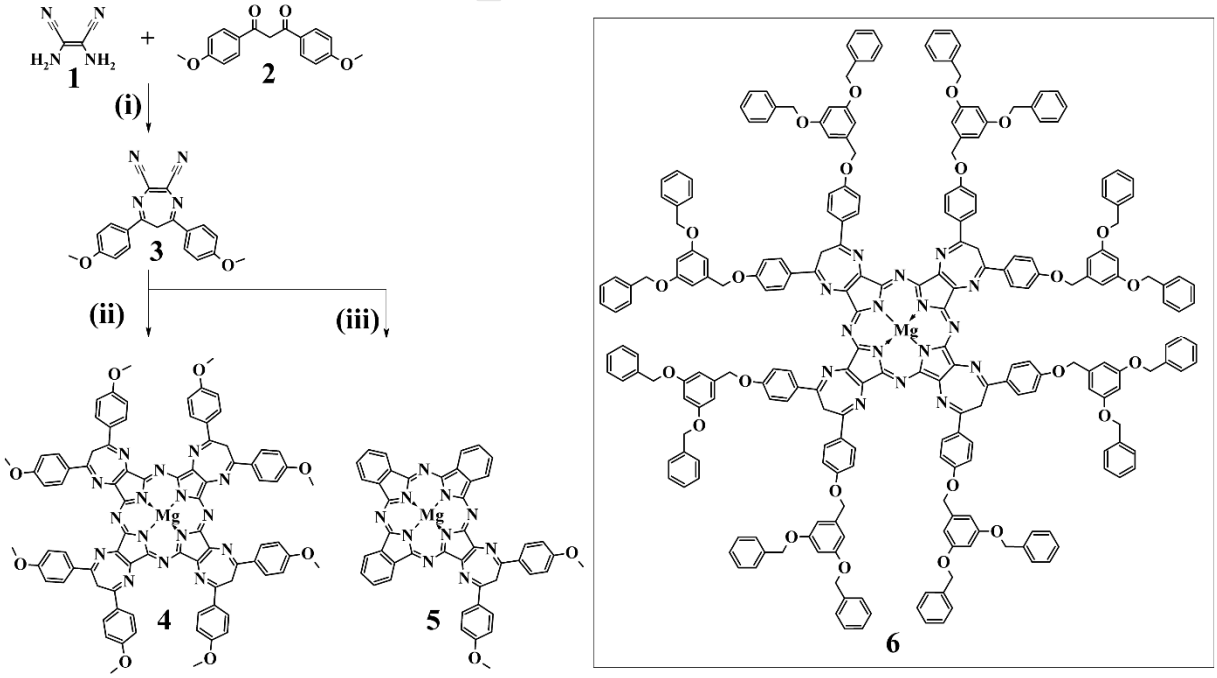

Scheme 1. Synthesis of porphyrazines **4** and **5**. Reagents and conditions: (i) ethanol, P_2O_5, reflux, 10 h, (60%); (ii) Mg(O*n*Bu)$_2$, *n*BuOH, reflux, 20 h, (10%); (iii) 1,2-dicyanobenzene, Mg(O*n*Bu)$_2$, *n*BuOH, reflux, 20 h, (3.5%).

2.2. Photochemical studies

2.2.1. Absorption and emission

Photochemical properties of symmetrical porphyrazine **4** and tribenzoporphyrazine **5** were determined together with the previously obtained symmetrical G1-dendrimeric diazepinoporphyrazine **6** (Inset in Scheme 1).[12] Firstly, the absorption properties of **4** and **6** were evaluated in various protic and aprotic organic solvents. The selected UV-Vis spectra are shown in Fig. 1, whereas Table S4, included in the Supplementary Information presents the spectral data including the absorption maxima of the Soret- and Q-bands with the corresponding absorption coefficients. The electronic absorption spectra recorded in various solvents revealed broad intensive Soret bands with the maxima in the range 343–389 nm for **4** and 347–389 nm for **6** and broad Q-bands with maxima between 637-676 and 640-674 nm, respectively. Moreover, it was observed that in both symmetrical porphyrazines the Q-band split into two sub-bands of different intensities depending on the solvent applied. The presence of the additional band is connected with the above-described aggregation.

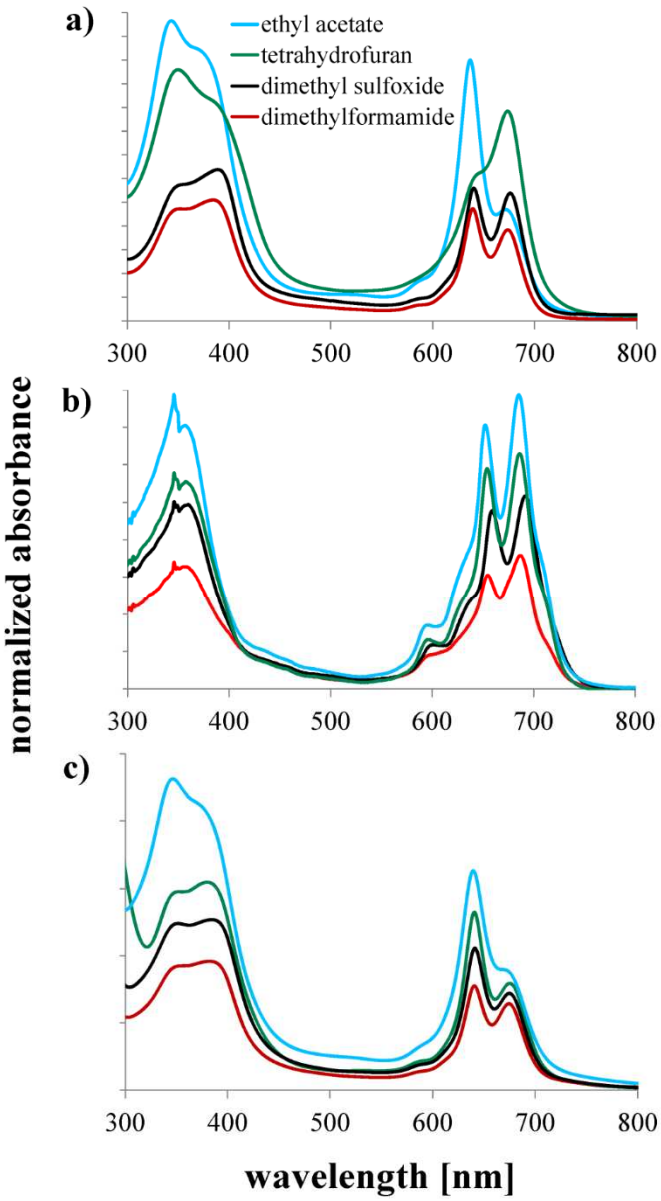

Fig. 1. Normalized absorption spectra of **4** (a), **5** (b) and **6** (c) in selected organic solvents.

The fluorescence emission spectra of **4**-**6** were recorded in dimethylformamide (DMF) and dimethylsulfoxide (DMSO) and are presented in Figure 2. Symmetrical porphyrazines **4** and **6** reveal fluorescence maxima at 681 nm in DMF and 682 nm in DMSO. In the spectrum of tribenzoporphyrazine **5**, split emission bands with maxima at 683 and 699 nm in DMF and 684 and 792 nm in DMSO can be noticed. The fluorescence quantum yield (Φ_F) values were calculated following the relative method proposed by Chauke *et al.*[25] with zinc(II) phthalocyanine (ZnPc) as a reference (Φ_F = 0.17 and 0.20 in DMF and DMSO, respectively). The tribenzoporphyrazine **5** revealed moderate fluorescence emission with Φ_F value of 0.19 in DMF and 0.16 in DMSO. The symmetrical porphyrazine **4** showed slightly intensive emission

with Φ_F = 0.17 in DMSO as compared to Φ_F = 0.16 in DMF. In both solvents, symmetrical G1-type dendrimeric porphyrazine **6** revealed less intense fluorescence with Φ_F equal to 0.12 and 0.13 in DMF and DMSO, respectively (Table 1).

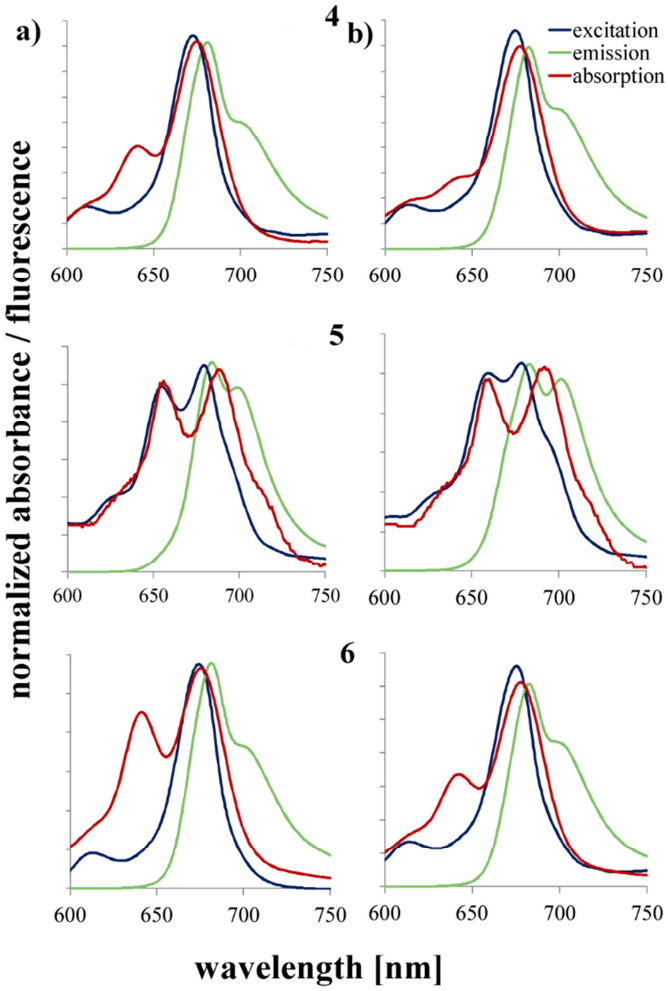

Fig. 2. The Q-band absorption, emission and excitation spectra of **4-6** in DMF (a) and DMSO (b).

2.2.2. Aggregation

Tendency to aggregation of porphyrazines **4-6** was evaluated in DMF and DMSO solutions following the Stuzhin *et al*. procedure.[6] Figure 3 and 4 present the changes in the UV-Vis spectra of porphyrazines **4-6** in DMF and DMSO after addition of 10% water and tetramethylammonium fluoride (TMAF) as an antiaggregation agent. On the one hand, the addition of water to the solution of **4** increases the intensity of the short wavelength sub-band with λ_{max} ~ 640 nm and decreases the intensity of the long wavelength band with λ_{max} ~ 675 nm. On the other hand, the addition of TMAF causes the disappearance of the short

wavelength band and only one single and intensive band with λ_{max} ~ 675 nm can be observed. The results confirmed that the long wavelength band corresponds to the monomeric form of porphyrazines, whereas the short wavelength band is a result of the formation of aggregates. Moreover, the fluorescence intensity increases after the addition of TMAF and decreases significantly when water is added, as it is well-known that aggregation is responsible for fluorescence quenching.[26,27] It was found that the aggregation tendency of **4** and **6** is strongly dependent on the solvent used. In the UV-Vis spectrum of **4** in DMF the bands for aggregated and monomeric species revealed similar intensity indicating strong aggregation, while for **6** only a residual band was observed as being the result of aggregates formation. It is worth noting that in DMSO the aggregation level was higher for **6** than for **4** (Figure 3 and 4). These data indicate that **4** and **5**, unlike **6**, aggregate in both DMF and DMSO. The aggregation of photosensitizers is a common problem for their further applications in photodynamic therapy (PDT), as the self-association of the photosensitizer molecules reduces the generation of singlet oxygen, thus hindering the photosensitizing efficiency.[28] For tribenzoporphyrazine **5**, with low symmetry molecules, a split band in the long-wavelength UV-Vis region was observed, which is known to be related to the symmetry reduction of π-chromophore.[3] Significant intensity of this band is a result of π – π* transitions in the macrocyclic system,[1,2,3,29] when going from a high symmetry to a low symmetry porphyrazine. As tribenzoporphyrazine macrocycle is unsymmetrical, the Q-band region is relatively broad and may overlap the n - π* transitions as a result of partial conjugation of N atom lone pairs of electrons of the boat-shaped diazepine rings in the 6*H*-form with the central π-chromophore. Detailed research performed by Ercolani and Stuzhin[2] on the group of symmetrical diazepinoporphyrazines indicated that the n – π* transitions can mix with the π – π* transitions and gain in intensity, which is reflected in the appearance of the Q-band. A spectral feature characteristic for diazepinoporphyrazines is an additional sub-band present in the Q-band region.

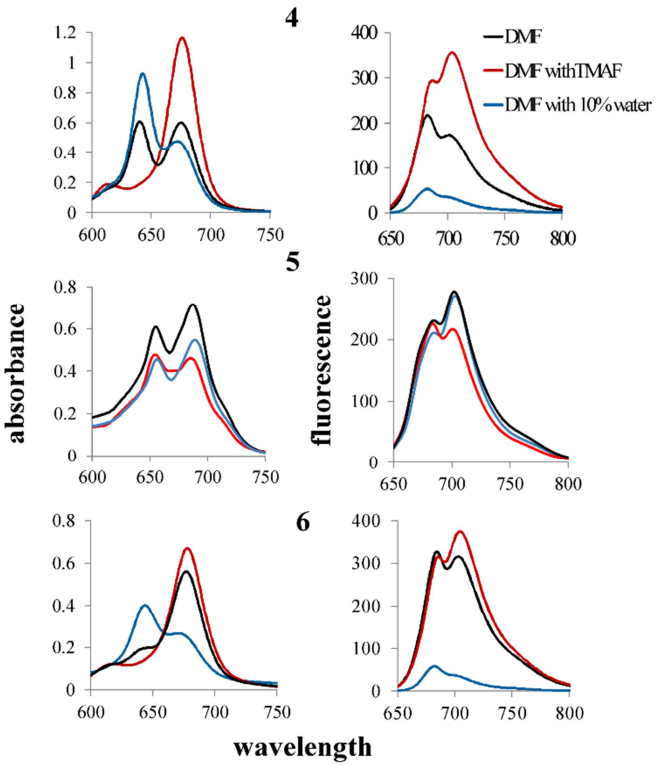

Fig. 3. Aggregation studies of **4-6** in DMF.

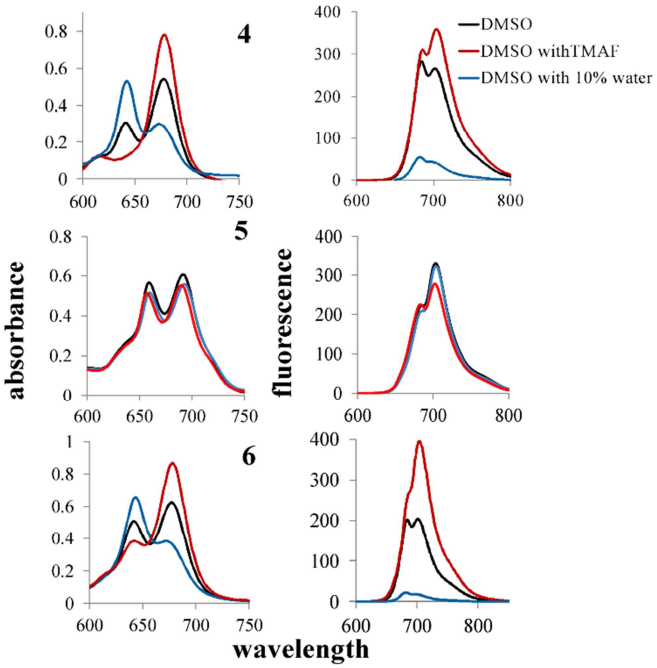

Fig. 4. Aggregation studies of **4-6** in DMSO. The absorption plots of **6** were published.[12]

2.2.3. Singlet oxygen generation

The potential photosensitizing activities of the obtained porphyrazines were evaluated by measuring their ability to generate singlet oxygen as a result of interaction between the activated photosensitizer and triplet oxygen. 1,3-Diphenylisobenzofuran (DPBF) was used as a chemical quencher, which undergoes a cycloaddition reaction with singlet oxygen to produce endoperoxide.[30] Solutions containing **4-6** or ZnPc in a mixture with DPBF in DMF or DMSO were irradiated with monochromatic light at the wavelengths corresponding to the Q-band maxima of their monomeric form. The kinetics of DPBF decomposition by photogenerated singlet oxygen was studied by monitoring decrease of the absorbance at 417 nm, and they were used to calculate the singlet oxygen generation yields (Φ_Δ). To determine the role of monomeric form of porphyrazines in singlet oxygen generation, the measurements for **4** and **6** were performed with and without the addition of TMAF. Table 1 presents the calculated values of singlet oxygen quantum yield for **4** and **6** in the presence and in the absence of TMAF. Moreover, changes in the UV–Vis spectra during irradiation of the solutions containing **4** or **6**, DPBF and TMAF in DMF or DMSO and the first-order plots of DPBF degradation by photogenerated singlet oxygen are shown in Figures S4-S8 in the Supporting Information. It was found that both symmetrical porphyrazines induce singlet oxygen formation better in DMSO than DMF. It is worth noting that **4** was the more efficient

singlet oxygen generator (with the Φ_Δ values at 0.078 and 0.249 in DMF and DMSO, respectively) than **6** (with the Φ_Δ values at 0.050 and 0.090 in DMF and DMSO, respectively). However, after the addition of TMAF, the Φ_Δ values for both porphyrazines were similar (0.307 in DMF, 0.295 in DMSO for **4**; 0.126 in DMF, 0.295 in DMSO for **6**), indicating that aggregation tendency can play a key role in the efficiency of singlet oxygen production. The lack of visible changes in the **4**-**6** Q-band absorptions proves the photostability of porphyrazines upon irradiation. The singlet oxygen generation yields of tribenzoporphyrazine **5** in DMF and DMSO were rather low or moderate with the Φ_Δ values at 0.069 and 0.180, respectively.

Table 1. Quantum yields of singlet oxygen production (Φ_Δ) and quantum yields of fluorescence emission (Φ_F) for **4** - **6**.

porphyrazine	$\Phi_\Delta \pm \Delta\Phi_\Delta$*		Φ_F	
	DMF	DMSO	DMF	DMSO
4	0.078 ± 0.003	0.249 ± 0.007	0.16	0.17
4 with TMAF	0.307 ± 0.011	0.295 ± 0.021	-	-
5	0.069 ± 0.001	0.180 ± 0.006	0.19	0.16
6	0.050 ± 0.002	0.090 ± 0.007**	0.12	0.13
6 with TMAF	0.126 ± 0.003	0.295 ± 0.024**	-	-

*results are given with 95% confidence

**values from ref.[12]

2.3. Liposomal formulations

Porphyrazines **4-6** are highly lipophilic. To increase their potential as photosensitizers for PDT applications, a proper drug-delivery system allowing further biological experiments in aqueous media is necessary.[31-36] With this goal in mind, liposomes containing porphyrazines were proposed. This approach seemed rational because liposomal nanoparticles have already been used as a drug delivery system for photosensitizers, enhancing their solubility in water and cell uptake.[37] Two different liposome formulations were prepared by a thin-film hydration method: (*i*) negatively charged liposomes composed of L-α-phosphatidyl-DL-glycerol (PG) and 1-palmitoyl-2-oleoyl-sn-glycero-3-phosphocholine (POPC) and (*ii*) positively charged liposomes containing 1,2-dioleoyl-3-trimethylammonium-propane (chloride salt, DOTAP) and POPC.[38,39]

The obtained liposomes were used as non-extruded, multilamellar vesicles, because the extrusion could reduce drug encapsulation, especially in the case of porphyrazine **6** with large, bulky substituents. Following Bhardwaj and Burgess study, it is worth noting that the sonication and extrusion of liposomes based on phosphatidylcholine derivatives have reduced dexamethasone encapsulation by approximately 50% in comparison to non-extruded liposomes.[40] The size of liposomes containing porphyrazines **4**-**6**, as well as blank liposomes, prepared as a control, was evaluated by dynamic light scattering method (Table S5 in the Supplementary Information). Two liposome fractions of different diameter were found for all formulations. The blank PG-POPC and DOTAP POPC liposomes were composed in about 11% of vesicles with the mean diameter varied from 40 to 50 nm, and in 89% of vesicles with the mean diameter in the range of 620-720 nm. Both liposomal formulations containing porphyrazine **4** were composed of vesicles with the mean diameter in the range of 60-70 and 540-590 nm, but the proportion of these two fractions was different. DOTAP-POPC-**4** liposomes contained 11% of smaller and 89% of larger nanoparticles, while PG-POPC-**4** about 37% of smaller and 63% of larger nanoparticles. Liposomes containing porphyrazine **5** were composed in 17-19% of vesicles with the mean diameter in the range 70-80 nm and in 81-83% of vesicles of the mean diameter of 400 nm. DOTAP-POPC-**6** liposomes were composed of vesicles with the mean diameter of 120 nm and 640 nm in 31% and 69%, respectively. PG-POPC-**6** liposomes were composed in about 10% of vesicles with the mean diameter of 540 nm, whereas in about 90% of vesicles with the mean diameter of 790 nm (Table S5 in Supplementary Information). No direct relationship between the size of liposomes and their compositions was found. However, liposomes containing porphyrazine **6** were larger than the others. Nevertheless, a further biological study towards an efficient method for the production of unilamellar and unified liposomes are necessary.

2.4. Anticancer assay (*in vitro* cellular studies)

The cytotoxicity of porphyrazines **4**-**6** to LNCaP cells was examined both in the presence and the absence of light using MTT assay (Figure 5).[41] It was found, that **4** did not exert any activity against cancer cells. Furthermore, it was observed that porphyrazine **4** incorporated into positively charged liposomes with DOTAP-POPC (DOTAP-POPC-**4**) displayed light-independent toxicity (the decrease of the cell viability to 70% and 65% in dark and light condition, respectively), whereas this effect was not seen for negatively charged liposomes with PG-POPC (PG-POPC-**4**). Additionally, we noted that DOTAP-POPC-**4** and **-6**

liposomes probably precipitate during incubation. To date, it was found that the electrolytes may reduce the positive charge of cationic lipids, e.g. phosphate buffer saline (PBS) has an additional effect of phosphate polyanions which tend to react and precipitate cationic liposomes.[42] Similarly, compound **6** appeared inactive and exhibited only slight cytotoxic effects at the highest tested dose (10μM) for DOTAP:POPC formulation in the dark and after High Power Multi Chip LEDs exposure (cell viability was around 80%).

In the dark condition porphyrazine **5** in its free form and after incorporation into liposomes DOTAP-POPC-**5**, PG-POPC-**5** was not cytotoxic in all tested concentrations, whereas in the light condition exhibited high cytotoxicity under irradiation with the dose of 2 J/cm^2. The cytotoxic effects increased along with the concentration for all formulations with the half maximal inhibitory concentration (IC_{50}) under the normoxic conditions at 0.814 ± 0.466 μM, 0.161 ± 0.002 μM and 0.166 ± 0.058 μM for **5**, DOTAP-POPC-**5**, and PG-POPC-**5**, respectively. Thus, as shown in Figure 5 the liposomal formulation may enhance cytotoxic activity of **5**. In general, the liposomal formulation prevents the aggregation of photosensitizers and in turn improves their activity.[43] Thus, a number of studies have shown that liposomal formulations of photosensitizers are more effective when compared to the free drug.[44-47] Based on the study results obtained under normoxic conditions, further evaluation of the activity of **5** was performed under hypoxia (defined as 1% of O_2). It is well-known that hypoxia may significantly affect the efficiency of PDT and for many years it has been considered a possible mechanism of resistance.[42] Taking into account that PDT works mainly by singlet oxygen generation and other reactive oxygen species (ROS), the concentration of oxygen is critical to the efficiency of PDT.[48,49] Moreover, hypoxia is one of the main features of solid tumors and has been associated with a poor clinical outcome of PDT.[50] Therefore, in order to gain more insight into the potential of **5** for photodynamic therapy, further biological evaluation of this compound was assessed in hypoxia conditions. Interestingly, all tested formulations remained photocytotoxic in hypoxia. However, the results indicated that **5** in liposomal formulation revealed better therapeutic effect than the free counterpart in hypoxia experiments (IC_{50} values of 3.135 ± 0.156 μM, 0.600 ± 0.357 μM and 0.378 ± 0.002 μM for **5**, DOTAP-POPC-**5**, and PG-POPC-**5**, respectively). Summarizing, *in vitro* experiments demonstrated that liposomal formulations of **5**, particularly PG-POPC-**5** may be considered as a promising photosensitizer for cancer treatment. However, further studies are necessary to fully evaluate the photodynamic potential of this compound.

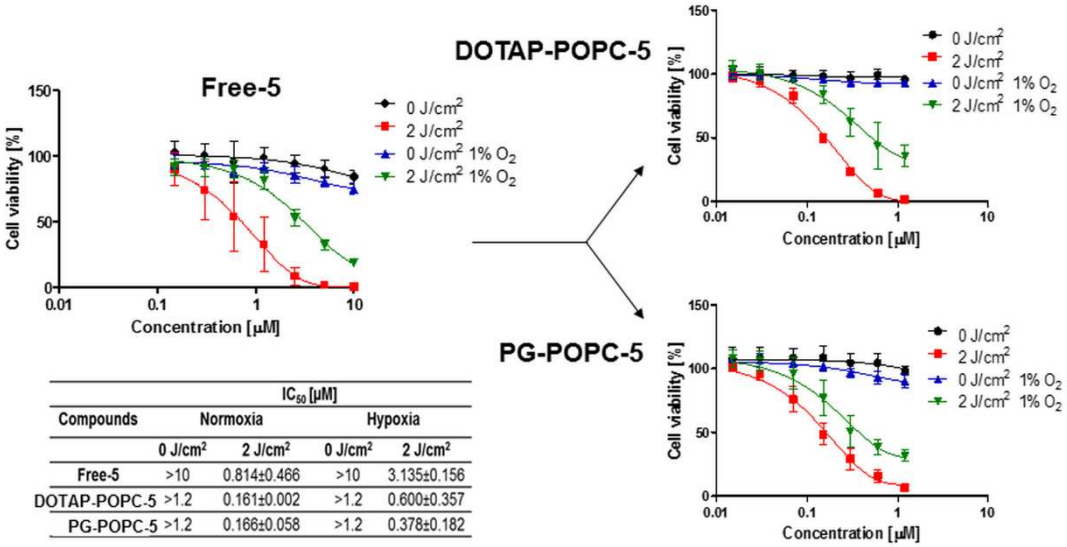

Compounds	IC_{50} [μM]			
	Normoxia		Hypoxia	
	0 J/cm²	2 J/cm²	0 J/cm²	2 J/cm²
Free-5	>10	0.814±0.466	>10	3.135±0.156
DOTAP-POPC-5	>1.2	0.161±0.002	>1.2	0.600±0.357
PG-POPC-5	>1.2	0.166±0.058	>1.2	0.378±0.182

Figure 5. Cytotoxicity of compound **5** and its two liposomal formulations (DOTAP-POPC and PG-POPC) against LNCaP cell line under normoxic and hypoxic conditions. Results are presented as a mean ± SD from two or three independent experiments. The table presents the IC_{50} values.

2.5. Antimicrobial activity

The photodynamic antimicrobial effect of novel macrocycles was investigated against *Staphylococcus aureus* ATCC 25923 and *Escherichia coli* ATCC 25922 – the representatives of both gram-positive and gram-negative bacteria, respectively. The antibacterial activity of porphyrazine **5** incorporated into two liposomal formulations as well as liposomes alone was studied in conditions of both dark and light.

Table 2. Bacterial reduction of planktonic *Staphylococcus aureus* ATCC 25923 and *Escherichia coli* ATCC 25922 in the presence of porphyrazine **5** in DOTAP-POPC or PG-POPC liposomes.

Bacterial strain		Log_{10} reduction in viable count ± SD*						
		Control	DOTAP-POPC-**5** at concentration [μM]		PG-POPC-**5** at concentration [μM]		DOTAP-POPC	PG-POPC
			5×10^{-5}	1×10^{-5}	5×10^{-5}	1×10^{-5}		
S. aureus ATCC 25923	Photo toxicity	0.25 ± 0.12	**2.07 ± 0.88**	0.48 ±0 .07	0.45 ± 0.12	0.86 ± 0.06	0.11 ± 0.11	0.01 ±0 .06
E. coli ATCC 25922		-0.06 ± 0.08	0.10 ± 0.18	NT	0.21 ± 0.18	NT	-0.15 ± 0.04	-0.16 ± 0.06
S. aureus ATCC 25923	Dark toxicity	NT	0.22 ± 0.03	-0.06 ± 0.06	0.08 ± 0.06	0.07 ± 0.13	0.14 ± 0.02	0.12 ± 0.01
E. coli ATCC 25922		NT	-0.02 ± 0.14	NT	-0.04 ± 0.14	NT	-0.01 ± 0.04	0.05 ± 0.16
Phototoxicity was assessed by calculating the phototoxic reduction factor - R_{Ph}= log L(-)Ps(-) – log L(+)Ps(+), whereas dark toxicity by calculating the dark toxic reduction factor - R_D= log L(-)Ps(-) – log L(-)Ps(+). For control the reduction factor was calculated as follows: $R_{Control}$= log L(-)Ps(-) – log L(+)Ps(-); L – light, Ps- photosensitizer								

As it was presented in the Table 2, an irradiation of planktonic bacterial strains in the presence of porphyrazine **5** in DOTAP-POPC liposomes at 5×10^{-5} μM (Ps+L+) significantly reduced CFUs of *Staphylococcus aureus* ATCC 25923 in comparison to **5** in PG-POPC liposomes, and the control liposomal formulations without photosensitizer (consisting of DOTAP-POPC or PG-POPC). However, insignificant reduction in cell survival was observed for **5** incorporated in DOTAP-POPC liposomes at a concentration of 1×10^{-5} μM and for **5** incorporated in PG-POPC liposomes at concentrations 5×10^{-5} and 1×10^{-5} μM. In addition, studied tribenzporphyrazine did not reveal any phototoxicity on *Escherichia coli* ATCC 25922 regardless of the liposomal formulation applied. It should be underlined that the tested liposome formulations did not reveal any influence on the microbes involved in research. Also, no dark toxicity on microorganisms after 20 minutes of exposure was noticed for either the tested photosensitizer or the liposomal formulations. Our results indicated that **5** incorporated into DOTAP-POPC liposomes revealed moderate phototoxicity for antibacterial photodynamic therapy.

3. Experimental

3.1. Materials and instruments

All reactions were conducted in oven-dried glassware under argon using Radleys Heat-On heating system. Solvents and all reagents were obtained from commercial suppliers and used without further purification. All solvents were removed by rotary evaporation at or

below 50 ºC. Dry flash column chromatography was carried out on Merck silica gel 60, particle size 40-63 µm, reverse phase Fluka C18 silica gel 90 and aluminum oxide 90 active neutral (activity stage I) for column chromatography 0.063-0.200 mm, EMD Millipore. Thin layer chromatography (TLC) was performed on silica gel Merck Kieselgel 60 F_{254} plates and Merck Kieselgel 60 RP-18 F_{254}s visualized with UV (λ_{max} 254 or 365 nm). All chromatography phases are given in volume to volume ratio. UV-Vis spectra were recorded on Hitachi UV/VIS U-1900 and Shimadzu UV-160A spectrophotometers. Melting points were obtained on a "Stuart" Bibby apparatus and are uncorrected. NMR spectra were acquired on an Agilent DD2 800 spectrometer at 298 K, unless stated otherwise. Chemical shifts (δ) are reported in parts per million (ppm) and referenced to the residual solvent peak (DMSO-d_6: δ_H = 2.50 ppm, δ_C = 39.5 ppm; pyridine-d_5: δ_H = 8.74, 7.58, 7.22 ppm, δ_C = 150.35, 135.91, 123.87 ppm). Coupling constants (*J*) are quoted in Hertz (Hz). The abbreviations s, d, dd, m, Ar, ax, eq, tribenzoH refer to singlet, doublet, doublet of doublets, multiplet, aromatic, axial, equatorial and tribenzoporphyrazine phenyl ring protons, respectively. ^{1}H and ^{13}C resonances were unambiguously assigned based on ^{1}H, ^{13}C, ^{1}H-^{1}H COSY, ^{1}H-^{13}C HSQC and ^{1}H-^{13}C HMBC experiments. Mass spectra (MS ES, MALDI TOF) and combustion analyses were carried out by the Advanced Chemical Equipment and Instrumentation Facility at the Faculty of Chemistry and the Wielkopolska Center for Advanced Technologies at Adam Mickiewicz University in Poznan. Tetrakis[5,7-bis-[4-[3,5-bis(benzyloxy)benzyloxy]phenyl]-6*H*-1,4-diazepino][2,3-b;2',3'-g;2'',3''-l;2''',3'''-q]porphyrazinato magnesium(II) was synthesized according to lately published procedure.[12]

3.2. Synthesis

2.2.1. 5,7-Bis(4-methoxyphenyl)-6*H*-1,4-diazepine-2,3-dicarbonitrile (3)

The reaction mixture containing diaminomaleonitrile **1** (0.38 g, 3.5 mmol), 1,3-bis(4-methoxyphenyl)-1,3-propanedione **2** (1 g, 3.5 mmol) and P_2O_5 (0.15 g, 1.56 mmol) in anhydrous ethanol (20 mL) was stirred for 1 h. After addition of further portion of P_2O_5 (0.15 g, 1.56 mmol), the reaction mixture was refluxed for 10 h. After the solvent was evaporated, the precipitate was filtered and washed with methanol to give yellow solid **3** (0.75 g, 60% yield). M.p. >250 °C dec. R_f (dichloromethane) 0.25. UV-Vis (dichloromethane): λ_{max}, nm (log ε) 378 (4.45), 314 (4.73). ^{1}H NMR (799.926 MHz, DMSO-d_6): δ_H, ppm 8.12 (d, 4H, ^3J=9 Hz, C2′, C6′, ArH), 7.01 (d, 4H, ^3J=9 Hz, C3′, C5′, ArH), 6.10 (d, 1H, ^2J=11 Hz, N=C-CH^{ax}), 3.82 (s, 6H, CH_3), 2.21 (d, 1H, ^2J=11 Hz, N=C-CH^{ax}). ^{13}C NMR (201.162 MHz, DMSO-d_6):

δ_C, ppm 163.2 (C4′, ArC), 150.2 (C1′, ArC), 132.7 (C2′, C6′, ArC), 125.6 (C=N), 122.8 (C≡N), 116.2 (C-C≡N), 114.5 (C3′, C5′, ArC), 55.6 (CH_3), 38.5 (C6). MS (ES pos) *m/z* 357 $[M+H]^+$, 379 $[M+Na]^+$, 395 $[M+K]^+$. MS (ES neg) *m/z* 355 $[M-H]^-$, 391 $[M+Cl]^-$. MS (MALDI) *m/z* found: 395.0920 $[M+K]^+$ calcd for 395.0910. Anal. calc. for $C_{21}H_{16}N_4O_2$: C, 70.77; H, 4.53; N, 15.72; O, 8.98; Found: C, 70.81; H, 4.52; N, 15.79; O, 8.88.

3.2.2. Tetrakis[5,7-bis(4-methoxyphenyl)-*6H*-1,4-diazepino][2,3-b;2’,3’-g;2’’,3’’-l;2’’’,3’’’-q]porphyrazinato magnesium(II) (4)

Magnesium turnings (16.8 mg, 0.7 mmol), a crystal of iodine, and in *n*-butanol (9 mL) were heated under reflux for 4 h. After the mixture was cooled to room temperature, maleonitrile derivative **3** (0.25 g, 0.7 mmol) was added and the reaction mixture was heated under reflux for 20 h. After being allowed to cool to room temperature, the reaction mixture was filtered through Celite which was further washed with toluene and dichloromethane. Filtrates were evaporated and the crude residue was subjected to column chromatography using silica gel (dichloromethane, dichloromethane:methanol, 20:1) and reversed-phase silica gel (methanol to dichloromethane:methanol, 2:1) to give the dark green product **4** (0.025 g, 10% yield). R_f (dichloromethane:methanol 20:1) 0.54. UV-Vis (dichloromethane): λ_{max}, nm (log ε) 270 (5.09), 348 (5.18), 650 (5.03), 676 (4.98). ^{1}H NMR (799.926 MHz, pyridine-d_5): δ_H, ppm 8.56 (d, 16H, ^3J=8.1 Hz, C2′, C6′, ArH), 6.89 (d, 16H, ^3J=8 Hz, C3′, C3′, ArH), 6.86 (d, 4H, ^2J=13 Hz, N=C-CH^{eq}), 6.07 (d, 4H, ^2J=13 Hz, N=C-CH^{ax}), 3.80 (s, 24H, CH_3). ^{13}C NMR (201.162 MHz, pyridine-d_5): δ_C, ppm 161.5 (C4′, ArC), 154.7, 145.8 (C1′, ArC), 142.6, 132.1 (C2′, C6′, ArC), 130.8 (N=C), 114.3 (C3′, C3′, ArH), 55.3 (CH_3), 37.1 (N=C-CH_2). MS (MALDI) *m/z* found: $[M+H]^+$ 1449.5000 calcd for 1449.5022. HPLC purity (see supplementary information).

3.2.3. 5,7-Bis(4-methoxyphenyl)-6*H*-1,4-diazepino[2,3-b]tribenzo[g,l,q]porphyrazinato magnesium(II) (5)

Magnesium turnings (0.075 g, 3.087 mmol), a crystal of iodine, and *n*-butanol (40 mL) were heated under reflux for 3 h. After the mixture was cooled to room temperature, **3** (0.2 g, 0.561 mmol) and 1,2-dicyanobenzene (0.719 g, 5.612 mmol) were added and reaction mixture was heated under reflux for a further 20 h. After being allowed to cool to room temperature, solvent was evaporated and the crude residue was washed with the mixture of water and methanol (1:1). After drying the solid was dissolved in dichloromethane and filtered through Celite. The filtrate was evaporated to dry residue, which was subjected to column chromatography using: (*i*) silica gel and eluents dichloromethane, dichloromethane/methanol

50:1, dichloromethane/methanol 20:1; (*ii*) Al_2O_3 and eluents dichloromethane, dichloromethane/methanol 200:1; (*iii*) C_{18}-reversed phase silica gel and eluents H_2O/methanol 3:1, dichloromethane/methanol 1:3; (*iv*) preparative TLC and eluents dichloromethane/methanol 10:1 and dichloromethane/pyridine 50:1 to give **5** as a deep green thin film (0.015 g, 3.5 % yield). Other macrocyclic products were also formed but could not be separately isolated (see Supplementary Information). R_f (dichloromethane:methanol 20:1) 0.47. UV–Vis (dichloromethane): λ_{max}, nm (log ε): 352 (5.44), 657 (5.24), 695 (5.31). ^{1}H NMR (799.926 MHz, DMSO-d_6): δ_H, ppm 9.46 (m, 4H, tribenzo-H), 9.38 (m, 2H, tribenzo-H), 8.55 (d, 4H, *J*=8.5 Hz, C3′, C5′, ArH), 8.27 (dd, 2H, *J*=5.6, 2.6 Hz, tribenzoH), 8.24 (m, 4H, tribenzo-H), 7.21 (d, 4H, *J*=8.7 Hz, C2′, C6′, ArH), 4.59 (m, 2H, CH_2), 3.94 (s, 6H, CH_3). ^{13}C NMR (201.162 MHz, DMSO-d_6): δ_C, ppm 165.0 (C4′), 158.2, 158.1, 156.3, 154.7, 149.7 (C1′), 143.5, 142.0, 141.8, 141.6, 141.5, 134.4 (C3′, C5′), 133.0, 132.9 (tribenzo-CH), 132.8, 132.6 (tribenzo-CH), 126.0, 125.9 (tribenzo-CH), 125.8 (tribenzo-CH), 117.6 (C2′, C6′), 58.7 (CH_3), 40.0 (CH_2). MS (MALDI) *m/z* found $[M+H]^+$ 765.2380 calcd for 765.2325. HPLC purity (see Supplementary Information).

3.3. Photochemical studies

All experiments were performed at ambient temperature. UV-Vis spectra were recorded in the range of 200-900 nm using Shimadzu UV-160A and Jasco V-530 spectrophotometers. The UV-Vis spectra of porphyrazines **4-6** were recorded in various solvents in the concentrations from 5×10^{-6} to 1×10^{-5} mol/dm^3.

The quantum yields of singlet oxygen generation were determined in DMSO and DMF solutions (3.0 mL, no oxygen bubbled) using the relative method with zinc(II) phthalocyanine (Sigma–Aldrich) and DPBF as a reference chemical quencher for singlet oxygen according to the previously described procedure.[8] Solutions of porphyrazines **4-6** or ZnPc in DMF and DMSO in the presence of DPBF were irradiated in a 1 cm path-length quartz cell (3 mL) with monochromatic light by a 150 W high-pressure Xe lamp (Optel) through a monochromator M250/1200/U. Light of two different wavelengths adjusted to the maxima of two sub-bands in the Q-band region was used (absorbance of the sensitizers ~ 0.5). Further experiments were performed after addition to the solutions of **4**, **6** with DPBF the antiaggregation agent, TMAF. As a result, single, unsplit Q-bands were observed. Thus irradiation was performed with one wavelength adjusted to the Q-band maximum. The concentration of DPBF was set at ~ 3×10^{-5}

mol L^{-1} to avoid chain reactions induced by DPBF in the presence of singlet oxygen.[51] The light intensity was set to 0.5 mW/cm^2 (Radiometer RD 0.2/2 with TD probe, Optel).

Fluorescence spectra were recorded using a Jasco 6200 spectrofluorometer. The fluorescence quantum yields were calculated using the equation: $\Phi_F = \Phi_{F\ reference} \times (F_{sample}/F_{reference}) \times (A_{reference}/A_{sample})$, where F and A correspond to the measured area under the emission peak and the absorbance at the excitation position (670 nm), respectively.[25] ZnPc was used as a reference (ΦF_{ZnPc} = 0.17 in DMF and 0.20 in DMSO).[52] The concentrations of porphyrazines **4** and **6** were about 1×10^{-6} and porphyrazine **5** about 5×10^{-7}.

The aggregation study was performed following the procedure proposed by Stuzhin *et al.*[6] To solutions of **4**-**6**, was added either an antiaggregation agent TMAF or water, which induces aggregation. Next the absorption and fluorescence spectra were recorded.

3.4. Liposome preparation

Porphyrazines **4**-**6** were tested in the liposomal formulations. Due to insolubility of **4** and **6** in polar solvents, these compounds were tested only in liposomal formulations while compound **5** was also tested in its free form. The liposomal formulations were stored in the dark at 4 °C. The photosensitizer **5** was diluted in DMSO (Sigma Aldrich) at the concentration 10 mM and stored in the dark at -20 °C. 1-Palmitoyl-2-oleoyl-sn-glycero-3-phosphocholine (POPC), L-α-phosphatidyl-DL-glycerol (chicken egg, PG) and 1,2-dioleoyl-3-trimethylammonium propane (chloride salt, DOTAP) were purchased from Avanti Polar Lipids Inc. Two different liposome formulations were prepared by a thin-film hydration method.[38,39] Appropriate amounts of the lipid stock solutions in chloroform (POPC - 25 mg/mL, PG - 25 mg/mL, DOTAP - 10 mg/mL) and photosensitizer (0.4 mg/mL) were placed in glass tubes, mixed and evaporated to dryness using a rotary evaporator. Films formed on the bottom of the glass tubes were dried overnight in a vacuum oven at room temperature to evaporate any remaining chloroform. Subsequently, the dried films were hydrated with PBS. The molar ratios of ingredients in final liposome formulations were: (i) porphyrazines **4**-**6** (0.1), PG (2), POPC (8); (ii) porphyrazines **4**-**6** (0.1), DOTAP (2), POPC (8). The liposome size was determined by dynamic light scattering measurements using a Malvern Zetasizer Nano ZS (Table S5 in Supporting Information). Samples were stored at 2-8 °C under argon and were protected from light. The final concentration of photosensitizer achieved in the liposome suspensions was 100 μM. Liposomes without photosensitizers were prepared as controls.

3.5. Photocytotoxicity in cultured cells

All experiments were carried out with the human prostate carcinoma cell line (LNCaP). The cell line was purchased from the European Collection of Cells Cultures (ECACC, Salisbury, UK) and cultured in Dulbecco modified Eagle medium without phenol red supplemented with 10% fetal bovine serum (FBS), 1% penicillin/streptomycin and 1% L-glutamine at 37 °C, in a humidified atmosphere containing 5% CO_2. The activity of tested compounds was examined under normoxic (21%) and hypoxic (1% O_2) conditions. For hypoxia treatment, the cells were first maintained in the standard normoxic incubator for few hours until the cells grew attached to the plates. Then, the cells were placed in the hypoxia workstation (Whitley H35 Hypoxystation, Don Whitley Scientific Limited, UK) filled with 1% O_2, 5% CO_2 and 94% N_2, at 70% humidity and 37 °C.

The light source for irradiation cells was the High Power Multi Chip LEDs, generating a wavelength of 660 nm (for compounds **4** and **6**) and 690 nm (for compound **5**). The power of illumination was measured by a radiometer device PM16-130 Power Meter with Slim Photodiode Sensor (ThorLabs). Due to precipitation of **4** and **6** in DMSO/water mixtures, these compounds were tested only in liposomal formulations while compound **5** was also tested in its free form. The photosensitizer **5** was diluted in DMSO (Sigma Aldrich) at the concentration 10 mM and stored in the dark at -20 °C.

Cytotoxic effect of the tested photosensitizers was determined by MTT assay[41] after light irradiation (phototoxicity) or without irradiation (dark toxicity). After placing the cells in the hypoxia workstation all procedures such as treatment with tested compounds, irradiation, and incubation after irradiation were performed in 1% of O_2. The cells were seeded at density 2×10^4 cell per well and allowed to attach overnight. Subsequently, the plates were washed twice with PBS, and the tested compound in a medium containing 2.5% FBS without phenol red was added at different concentrations for a 24 h incubation period. The viability tests were performed for concentrations: 0.15; 0.3; 0.6; 1.25; 2.5; 5 and 10 µM for compounds **4**, **5** (non-liposomal formulation; free-**5**) and **6**. The preliminary *in vitro* studies showed that the liposomal formulations of **5** (DOTAP-POPC-**5** and PG-POPC-**5**) exerted strong cytotoxic effects; therefore, the tested concentrations for these compounds were decreased to 0.015; 0.03; 0.07; 0.15; 0.3; 0.6 and 1.2 µM. For the liposomal formulation of porphyrazines **4**-**6**, the liposomes without photosensitizers were prepared and used as the negative controls. For free-**5**, DMSO was used as a control, and the concentration in medium did not exceed 0.1%. After

incubation, the plates were washed twice with PBS, and fresh medium was added to each well. The cells were immediately light irradiated at light dose 2 J/cm^2 or not irradiated as the dark control plates. The cell viability was determined after 24 h using the MTT assay. Briefly, 170 µL of culture medium containing methylthiazolydiphenyl-tetrazolium bromide (Sigma Aldrich) solution (20 µL; 5 mg/ml PBS) was added to each well. Then, the cells were incubated for 2 h under cell culture condition, and the plates were centrifuged (1200 rpm, 3 min). The MTT solution was removed and the formazan crystals were dissolved by using 200 µl DMSO (Avantor Performance Materials S.A. Gliwice, Poland). The absorbance was measured at 570 nm with a plate reader (Elx-800, Biotek Instruments Winooski, VT, USA). The data were normalized to the mean absorption of control cells. All experiments were performed in duplicate, except the experiments for free-**5**, which were performed in triplicate.

3.6. Antimicrobial assay

The standard bacterial strains used in this study were *Staphylococcus aureus* ATCC 25923 and *Escherichia coli* ATCC 25922 and were obtained from the American Type Culture Collection (ATCC). The strains of bacteria were stored in Microbank cryogenic vials (ProLabDiagnostics, Canada) at -70 ± 10 °C. Microbes used for the study were plated on Tryptone Soya Agar (TSA; Oxoid, UK) and incubated at 36±1ºC for 18 h. Bacterial strains were cultured in the Brain Heart Infusion broth (BHI, Oxoid, UK) at 36 ± 1 °C for 18 h. Each culture was harvested by centrifugation (3000 × g for 15 min) and re-suspended in 1.5 mL of 10 mMPBS, pH, 7.0 (Sigma-Aldrich). The cells were then diluted 1/100 in PBS to a final concentration of about 10^7 colony forming units (CFU)/mL. Antibacterial photodynamic activity of the tested compounds was determined using suspension method as described previously.[53] Briefly, bacterial suspensions were incubated in the dark with the appropriate concentrations of 10 and 50 µM at room temperature for 20 min. After that, the samples were illuminated with the light intensity at the surface of the plate set to 5.0 mW/cm^2 (measured by Radiometer RD 0.2/2 with TD probe, Optel) and the total light dose was 18 J/cm^2 (group [L+, Ps+]). In parallel, three control experiments were designed as follows: (*i*) non-illuminated, no photosensitizer– [L(-), Ps(-)], (*ii*) non-illuminated, but with photosensitizer [L(-), Ps(+)], (*iii*) without photosensitizer, but illuminated [L(+), Ps(-)]. Cell viability of the samples was determined by serial dilution in PBS and then plated on TSA medium. After incubation of the plates at 36 ± 1°C for 24 h, the number of CFU per ml was counted, and the $\log_{10}$ reduction factor in microbial cells for each sample were calculated.

4. Conclusions

Novel 5,7-diaryl-substituted symmetrical diazepinoporphyrazine and tribenzodiazepinoporphyrazine were found to generate singlet oxygen in dimethylformamide and dimethyl sulfoxide in moderate yields up to 0.307 in comparison to structurally similar G1-dendrimeric diazepinoporphyrazine. Absorbance and fluorescence measurements that were applied to study aggregation properties of novel macrocycles in the presence of tetramethylammonium fluoride as an antiaggregation agent proved that the synthesized porphyrinoids are prone to aggregation.

The cytotoxicity of all porphyrazines to LNCaP cells was examined in both the presence and the absence of light using MTT assay. Symmetrical magnesium(II) diazepinoporphyrazine substituted at C5 and C7 positions with 4-methoxyphenyl groups did not exert any activity against cancer cells. Furthermore, this molecule incorporated into positively charged liposomes with DOTAP-POPC displayed light-independent toxicity, whereas this effect was not observed for negatively charged liposomes with PG-POPC. Similarly, symmetrical magnesium porphyrazine substituted at C5 and C7 positions with 4-[3,5-bis(benzyloxy)benzyloxy]phenyl substituents was found to be inactive and exhibited only slight cytotoxic effects at the highest tested dose (10 μM) for DOTAP-POPC formulation in the dark and after laser exposure. Also, it was observed that DOTAP-POPC liposomes containing both symmetrical porphyrazines probably precipitate during incubation.

Oxygen depletion in tumor tissue is a significant factor limiting numerous anticancer strategies including PDT. In our further studies, a free form of tribenzoporphyrazine substituted at C5 and C7 positions with 4-methoxyphenyl groups and its two liposomal formulations in DOTAP-POPC and PG-POPC were tested under normoxic and hypoxic (1% O_2) conditions against LNCaP cell line. In the dark condition, tribenzodiazepinoporphyrazine was not cytotoxic at all tested concentrations, whereas in the light condition it exhibited high cytotoxicity under irradiation with the dose of 2 J/cm^2. The cytotoxic effects of tribenzodiazepinoporphyrazine increased along with the concentration for all formulations with the half maximal inhibitory concentration (IC_{50}) under the normoxic conditions at 0.814 ± 0.466 μM, in DOTAP-POPC liposomes at 0.161 ± 0.002 μM and in PG-POPC liposomes at 0.166 ± 0.058 μM. It is interesting that all tested liposome formulations of tribenzoporphyrazine maintained their photocytotoxicity in hypoxia. Moreover, tribenzodiazepinoporphyrazine incorporated into liposomes revealed better therapeutic effect

(IC_{50} values of 0.600 ± 0.357 μM and 0.378 ±0.002 μM) than in its free form (IC_{50} values of 3.135 ± 0.156 μM). According to the *in vitro* experiments, L-α-phosphatidyl-DL-glycerol liposomal formulation was found the most promising for further study. It is worth noting that IC_{50} values obtained in hypoxic conditions for tribenzoporphyrazine formulations in DOTAP-POPC and PG-POPC were 2.7 – 3.7 higher than those found in normoxic conditions. However, it should be emphasized that even in heavy hypoxic conditions the obtained IC_{50} values are still much below the concentration value of 1 μM. It seems that further *in vitro* and *in vivo* studies are necessary to evaluate fully the usefulness of DOTAP-POPC and PG-POPC formulations of tribenzoporphyrazine substituted at C5 and C7 positions with 4-methoxyphenyl groups in photodynamic therapy of cancer.

Tribenzoporphyrazine incorporated into DOTAP-POPC liposomes revealed moderate phototoxicity for antibacterial photodynamic therapy. It was found that irradiation of planktonic bacterial strains in the presence of tribenzoporphyrazine in DOTAP-POPC liposomes at 5×10^{-5} μM significantly reduced CFUs of *Staphylococcus aureus* ATCC 25923 in comparison to tribenzoporphyrazine in PG-POPC liposomes, and the control liposomal formulations without photosensitizer. It is interesting that studied macrocycle did not reveal any phototoxicity on *Escherichia coli* ATCC 25922 regardless the liposomal formulation.

Acknowledgement

This study was supported by the National Science Centre, Poland under Grant No. 2012/05/E/NZ7/01204.

Appendix A. Supplementary data

Supplementary data associated with this article can be found in the online version, at doi:.....

References

1. S. Angeloni, C. Ercolani. *J. Porphyr. Phthalocya.* **2000**, *4*, 474–483.
2. M.P. Donzello, D. Dini, G. D'Arcangelo, C. Ercolani, R. Zhan, Z. Ou, P.A. Stuzhin, K.M. Kadish. *J. Am. Chem. Soc*. **2003**, *125*, 14190–14204.
3. M.P. Donzello, C. Ercolani, L. Mannina, E. Viola, A. Bubnova, O. Khelevina, P.A. Stuzhin. *Aust. J. Chem*. **2008**, *61*, 262–272.
4. S.M. Baum, A.A. Tabanco, A.G. Montalban, A.S. Micallef, C. Zhong, H.G. Meunier, K. Suhling, D. Phillips, A.J.P. Wite, D.J. Williams, A.G.M. Barret, B.M. Hoffman. *J. Org. Chem*. **2003,** *68*, 1664–1670.
5. T. Goslinski, J. Piskorz, D. Brudnicki, A.J.P. White, M. Gdaniec, W. Szczolko, E. Tykarska. *Polyhedron* **2011**, *30*, 1004–1011.
6. P.A. Stuzhin, P. Tarakanov, S. Shiryaeva, A. Zimenkova, O.I. Koifman, E. Viola, M.P. Donzello, C. Ercolani. *J. Porphyr. Phthalocya.* **2012**, *16*, 968–976.
7. J. Piskorz, E. Tykarska, M. Gdaniec, T. Gośliński, J. Mielcarek. *Inorg. Chem. Commun.* **2012**, *20*, 13–17.
8. J. Piskorz, K. Konopka, N. Düzgüneş, Z. Gdaniec, J. Mielcarek, T. Goslinski. *ChemMedChem* **2014,** *9* 1775–1782.
9. P.A. Tarakanov, M.P. Donzello, O.I. Koifman, P.A. Stuzhin. *Macroheterocycles* **2011**, *4*, 177–183.
10. P.A. Tarakanov, A.O. Simakov, A.Y. Tolbin, I.O. Balashova, V.I. Shestov, L.G. Tomilova. *Spectrochim. Acta A* **2015**, *139*, 464–470.
11. E.N. Tarakanova, S.A. Trashin, P.A. Tarakanov, V.E. Pushkarev, L.G. Tomilova. *Dyes Pigments* **2015**, *117*, 61–63.
12. E. Wieczorek, J. Piskorz, L. Popenda, S. Jurga, J. Mielcarek, T. Goslinski. *Tetrahedron Lett.* **2017**, *58*, 758–761.
13. P. Agostinis, K. Berg, K.A. Cengel, T.H. Foster, A.W. Girotti, S.O. Gollnick, S.M. Hahn, M.R. Hamblin, A. Juzeniene, D. Kessel, M. Korbelik, J. Moan, P. Mroz, D. Nowis, J. Piette, B.C. Wilson, J. Golab. *CA-Cancer J. Clin.* **2011**, *61*, 250–281.
14. D.S. Pellosi, P. da Costa Carvalho De Jesus, A.C. Tedesco. *Expert Opin. Drug Del*. **2017**, *14*, 1395-1406.
15. B.Q. Spring, I. Rizvi, N. Xu, T. Hasan. *Photochem. Photobiol. Sci*. **2015**, *14*, 1476–1491.
16. W. Fan, P. Huang, X. Chen. *Chem. Soc. Rev*. **2016**, *45*, 6488–6519.
17. M. Höckel, P. Vaupel. *J. Natl. Cancer Inst*. **2001**, *93*, 266–276.
18. S. Anand, B.J. Ortel, S.P. Pereira, T. Hasan, E.V. Maytin. *Cancer Lett*. **2012**, *326*, 8–16.
19. B. Li, L. Lin, H. Lin, B.C. Wilson. *J. Biophotonics* **2016**, *9*, 1314–1325.
20. J. Dang, H. He, D. Chen, L. Yin. *Biomater. Sci*. **2017**, *5*, 1500–1511.
21. S.R. McKeown. *Br. J. Radiol*. **2014**, *87*, 20130676.
22. C. Michiels, C. Tellier, O. Feron. *BBA - Rev. Cancer* **2016**, *1866*, 76–86.
23. N.J. Rupp, P.J. Schüffler, Q. Zhong, F. Falkner, M. Rechsteiner, J.H. Rüschoff, C. Fankhauser, M. Drach, R. Largo, M. Tremp, C. Poyet, T. Sulser, G. Kristiansen, H. Moch, J. Buhmann, M. Müntener, P.J. Wild. *J. Pathol. Inform*. **2016**, *7*, 3. doi: 10.4103/2153-3539.175376.
24. R.P. Linstead, M. Whalley. *J. Chem. Soc*. **1952**, 4839–4846.
25. V. Chauke, M. Durmuş, T. Nyokong. *J. Photochem. Photobiol. A* **2007**, *192*, 179–187.
26. A.T. Bilgiçli, M.N. Yaraşir, M. Kandaz, A. Rıza Özkaya. *Polyhedron* **2010**, *29*, 2498–2510.
27. M. Çamur, M. Bulut, M. Kandaz, O. Güney. *Polyhedron* **2009**, *28*, 233–238.

28. A.P. Castano, T.N. Demidova, M.R. Hamblin. *Photodiagn. Photodyn. Ther*. **2004**, *1*, 279–293.
29. S.L.J. Michel, S.M. Baum, A.G.M. Barrett, B.M. Hoffman in *Prog. Inorg. Chem.*; Karlin, K.D. (Ed.); J. Wiley & Sons, New York, 2001, vol. 50, pp.473–590.
30. I. Seotsanyana-Mokhosi, N. Kuznetsova, T. Nyokong. *J. Photochem. Photobiol. A* **2001**, *140*, 215–222.
31. J.M. Dąbrowski, B. Pucelik, A. Regiel-Futyra, M. Brindell, O. Mazuryk, A. Kyzioł, G. Stochel, W. Macyk, L.G. Arnaut. *Coord. Chem. Rev*. **2016**, *325*, 67-101.
32. Z. Jiang, J. Shao, T. Yang, J. Wang, L. Jia. *J. Pharm. Biomed. Anal*. **2014**, *87*, 98–104.
33. K. Lang, J. Mosinger, D.M. Wagnerová. *Coord. Chem. Rev*. **2004**, *248*, 321–350.
34. S. Md, S. Haque, T. Madheswaran, F. Zeeshan, V. Srikanth Meka, A.K. Radhakrishnan, P. Kesharwani. *Drug Discov. Today* **2017**, *22*, 1274–1283.
35. E.S. Nyman, P.H. Hynninen. *J. Photochem. Photobiol. B* **2004**, *73*, 1–28.
36. R. Weijer, M. Broekgaarden, M. Kos, R. van Vught, E.A.J. Rauws, E. Breukink, T.M. van Gulik, G. Storm, M. Heger. *J. Photochem. Photobiol. C* **2015**, *23*, 103–131.
37. P. Skupin-Mrugalska, J. Piskorz, T. Goslinski, J. Mielcarek, K. Konopka, N. Düzgünes. *Drug Discov. Today* **2013**, *18*, 776–784.
38. N. Düzgünes. *Methods Enzymol*. **2003**, *367*, 23–27.
39. M. Kryjewski, E. Tykarska, T. Rebis, J. Dlugaszewska, M. Ratajczak, A. Teubert, J. Gapinski, A. Patkowski, J. Piskorz, G. Milczarek, M. Gdaniec, T. Goslinski, J. Mielcarek. *Polyhedron* **2015**, *98*, 217–223.
40. U. Bhardwaj, D.J. Burgess. *Int. J. Pharm*. 2010, *388*, 181–189.
41. H. Zhao, R. Yin, D. Chen, J. Ren, Y. Wang, J. Zhanga, H. Deng, Y. Wang, H. Qiu, N. Huang, Q. Zou, J. Zhao, Y. Gu. *Photodiagn. Photodyn. Ther*. **2014**, *11*, 204–212.
42. L.H. Li, S.W. Hui. *Biochim. Biophys. Acta BBA - Biomembr*. **1997**, *1323*, 105–116.
43. T.A. Debele, S. Peng, T. Hsieh-Chih. *Int. J. Mol. Sci*. **2015**, *16*, 22094–22136.
44. K.H. Choi, C.W. Chung, C.H. Kim, D.H. Kim, Y.I. Young, D.H. Kang. *J. Nanosci. Nanotechnol*. **2014**, *14*, 5628–5632.
45. J. Young, M. Yee, H. Kim, J. Cheung, T. Chino, N. Düzgünes, K. Konopka. *Med. Sci. Monit. Basic Res*. **2016**, *22*, 156–164.
46. P.H. Guelluy, M.P. Fontaine-Aupart, A. Grammenos, S. Lécart, J. Piette, M. Hoebeke. *Photochem. Photobiol. Sci*. **2010**, *9*, 1252–1260.
47. Y. Sadzuka, K. Tokutomi, F. Iwasaki, I. Sugiyama, T. Hirano, H. Konno, N. Oku, T. Sonobe. *Cancer Lett*. **2006**, *241*, 42–48.
48. B.Q. Spring, I. Rizvi, N. Xu, T. Hasan. *Photochem. Photobiol. Sci.* **2015**, *14*, 1476–1491.
49. J. Dang, H. He, D. Chen, L. Yin. *Biomater. Sci*. **2017**, *5*, 1500–1511
50. C.T. Lee, M.K. Boss, M.W. Dewhirst. *Antioxid. Redox Signal* **2014**, *21*, 313–337
51. M. Durmuş, V. Ahsen, T. Nyokong. *J. Photochem. Photobiol. A* **2007**, *186*, 323–329.
52. A. Ogunsipe, D. Maree, T. Nyokong. *J. Mol. Struct*. **2003**, *650*, 131–140.
53. J. Dlugaszewska, W. Szczolko, T. Koczorowski, P. Skupin-Mrugalska, A. Teubert, K. Konopka, M. Kucinska, M. Murias, N. Düzgüneş, J. Mielcarek, T. Goslinski. *J. Inorg. Biochem*. **2017**, *172*, 67–79.

Porphyrazine derivatives were synthesized and characterized

Singlet oxygen generation and aggregation properties of porphyrazines were evaluated

Photocytotoxicity of porphyrazines was examined in free form and in liposomes

Photocytotoxicity of porphyrazines was studied under normoxic and hypoxic conditions